Quark orbital angular momentum from lattice QCD

N. Mathur,[1,2] S. J. Dong,[1] K. F. Liu,[1,3] L. Mankiewicz,[4,5] and N. C. Mukhopadhyay[2]
[1]*Department of Physics and Astronomy, University of Kentucky, Lexington, Kentucky 40506*
[2]*Department of Physics, Applied Physics and Astronomy, RPI, Troy, New York 12180*
[3]*SLAC, P.O. Box 4349, Stanford, California 94309*
[4]*Copernicus Astronomical Center, ul. Bartycka 18, PL-00-716 Warsaw, Poland*
[5]Andrzej Sołtan Institute for Nuclear Studies, Warsaw, Poland
(Received 10 December 1999; published 25 October 2000)

We calculate the quark orbital angular momentum of the nucleon from the quark energy-momentum tensor form factors on the lattice with the quenched approximation. The disconnected insertion is estimated stochastically which employs the Z_2 noise with an unbiased subtraction. This reduced the error by a factor of 3–4 with negligible overhead. The total quark contribution to the proton spin is found to be 0.30 ± 0.07. From this and the quark spin content we deduce the quark orbital angular momentum to be 0.17 ± 0.06 which is $\sim$34% of the proton spin. We further predict that the gluon angular momentum is 0.20 ± 0.07; i.e., $\sim$40% of the proton spin is due to the glue.

PACS number(s): 12.38.Gc, 13.88.+e, 14.20.Dh

I. INTRODUCTION

The spin content of the proton remains a challenging problem in QCD both experimentally and theoretically [1]. The surprisingly small contribution from the quark spin revealed by the polarized deep inelastic scattering experiments [2] (world average: $\Sigma=0.25\pm0.10$) has stimulated a great deal of interest in the understanding of this ''proton spin problem.'' While the lattice QCD calculations [3] confirmed the small quark spin content in agreement with experiments, there is little consensus on where the rest of the proton spin resides. There have been suggestions based on the Bjorken sum rule [4], the parton evolution [5], the chiral quark model [6], and the Skyrmion [7] that the quark orbital angular momentum in the nucleon can be substantial. It is further proposed that the off-forward parton distributions from deeply virtual Compton scattering can be used to measure the quark orbital angular momentum distribution and thereby its moments [8].

In this paper, we shall report the first lattice calculation of the quark energy-momentum tensor form factors which admits the extraction of the total quark angular momentum. Combining the lattice calculation of the quark spin content [3], we obtain the quark orbital angular momentum and thereby predict the gluon angular momentum in the nucleon from the spin sum rule. It turns out that the quark orbital angular momentum is indeed quite large. It constitutes $\sim$35% of the proton spin and the gluon angular momentum is predicted to make up the remaining $\sim$40% of the proton spin. We should point out the caveat that the present result is based on the quenched approximation and is subjected to correction when dynamical fermion is included. The formalism to extract quark angular momentum is given in Sec. II. The lattice calculation is presented in Sec. III and the conclusions are in Sec. IV.

II. FORMALISM

It has been shown recently [8] that the total angular momentum in QCD can be decomposed into three pieces in a *gauge invariant* way

$$\begin{aligned}\vec{J}&=\int d^3x\,\frac{1}{2}\bar{\psi}\vec{\gamma}\gamma_5\psi+\int d^3x\,\bar{\psi}\gamma_4\{\vec{x}\times(-i\vec{D})\}\psi\\&\quad+\int d^3x\,[\,\vec{x}\times(\vec{E}\times\vec{B})\,]\\&=\frac{1}{2}\vec{\Sigma}+\vec{L}_q+\vec{J}_g.\end{aligned}\tag{1}$$

The quark spin contribution $\frac{1}{2}\Sigma$ is defined through the forward matrix element of the flavor-singlet axial-vector current. Similarly, L_q, the quark orbital angular momentum, is defined from the operator $\vec{L}_q$ and J_g, the gluon angular momentum, is defined from $\vec{J}_g$ which is associated with the gluon Poynting vector $\vec{E}\times\vec{B}$. The total quark angular momentum is $J_q=\frac{1}{2}\Sigma+L_q$. Whereas, the total gluon angular momentum J_g cannot be further decomposed into gluon spin and gluon orbital angular momentum without explicit gauge dependence.

J_q can be obtained from the energy-momentum tensor form factors [8]. One can write the gauge invariant quark-gluon energy-momentum tensor as

$$T_{\mu\nu}=T^q_{\mu\nu}+T^g_{\mu\nu}=\frac{1}{2}\bar{\psi}\gamma_{(\mu}[\vec{D}-\overleftarrow{D}]_{\nu)}\psi+F_{\mu\alpha}F_{\nu\alpha}-\frac{1}{4}\delta_{\mu\nu}F^2,\tag{2}$$

where the first part is the quark energy-momentum tensor and the second one is that of the gluon. Form factors of the energy-momentum tensor for either the quark or the gluon are defined by [8]

$$\begin{aligned}&\langle p,s|T_{\mu\nu}(0)|p',s'\rangle\\&\quad=\bar{u}(p,s)\Big[T_1(q^2)\,i\gamma_{(\mu}\bar{p}_{\nu)}-T_2(q^2)\bar{p}_{(\mu}i\sigma_{\nu)\alpha}q_\alpha/2m_N\\&\qquad+\frac{1}{m_N}T_3(q^2)(q_\mu q_\nu-\delta_{\mu\nu}q^2)\\&\qquad-m_N T_4(q^2)\delta_{\mu\nu}\Big]u(p',s'),\end{aligned}\tag{3}$$

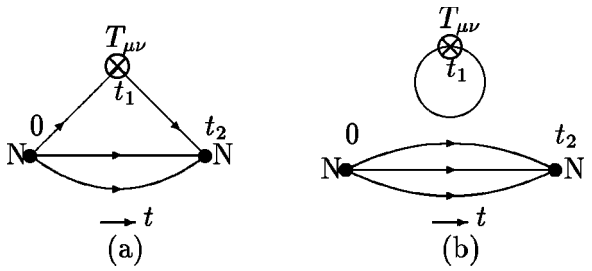

FIG. 1. Quark skeleton diagrams for the three-point function $G_{NT_{4j}N}(t_2,t_1,\vec{p},-\vec{q})$. (a) is the connected insertion. (b) is the disconnected insertion.

where $\overline{p}_\mu=(p_\mu+p'_\mu)/2$, $q_\mu=p_\mu-p'_\mu$ and $u(p)$ is the nucleon spinor. It can be proven that, for polarized target, the total angular momentum of the quarks or gluons is

$$J_{q,g}=\frac{\langle p,s|\,\frac{1}{2}\,\epsilon^{ijk}\int d^3x\,(T^{q,g}_{4k}x_j-T^{q,g}_{4j}x_k)\,|p,s\rangle}{\langle p,s|p,s\rangle}$$

$$=\frac{1}{2}[T_1^{q,g}(0)+T_2^{q,g}(0)]. \tag{4}$$

Therefore, the total angular momentum of the quarks or gluons can be calculated at the $q^2\to 0$ limit of the form factor $1/2[T_1^{q,g}(q^2)+T_2^{q,g}(q^2)]$.

III. LATTICE CALCULATION

In Eq. (3), the energy momentum tensor is expressed in terms of four form factors; whereas, for calculating the angular momentum we need only two, namely T_1 and T_2. T_{4j}, with j in the 3-direction, does not admit the T_4 term. To remove T_3, we choose the momentum transfer to be orthogonal to the j direction. In order to get the required $T_1(q^2)+T_2(q^2)$, we calculate the three point function $G_{NT_{4j}N}(t_2,t_1,\vec{p},-\vec{q})$ for the operator T_{4j}. The three point function has two parts: connected insertion (CI), due to the valence and connected sea quarks, and disconnected insertion (DI) attributed to the disconnected sea quarks [9] (Fig. 1).

For CI, we express the observable $T(q^2)\equiv\frac{1}{2}[T_1(q^2)+T_2(q^2)]$ in terms of the ratio of three- and two-point functions:

$$\frac{\mathrm{Tr}[\Gamma_m G_{NT_{4j}N}(t_2,t_1,\vec{0},-\vec{q})]}{\mathrm{Tr}[\Gamma_e G_{NN}(t_2,\vec{0})]}\,\frac{\mathrm{Tr}[\Gamma_e G_{NN}(t_1,\vec{0})]}{\mathrm{Tr}[\Gamma_e G_{NN}(t_1,\vec{q})]}$$

$$=\frac{1}{2}\epsilon_{jkm}\,q_k\,T(q^2), \tag{5}$$

where Γ_m and Γ_e are the spin polarized and unpolarized projection operators [10]. From the above ratio, we calculate the lattice $T_{CI}(q^2)$ at different q^2 and then extrapolate them to $q^2\to 0$ limit to obtain the CI part of the lattice quark total angular momentum $J_{q,CI}$. Results are obtained for relatively light Wilson quarks with $\kappa=0.148$, 0.152, 0.154 and 0.155. The dimensionless nucleon masses $M_N a$ for these κ values are 1.15(1), 0.882(12), 0.738(16), and 0.670(15), respectively. The corresponding dimensionless pion masses $m_\pi a$ are 0.679(4), 0.486(5), 0.376(6), and 0.304(12). Extrapolating the nucleon and pion masses to the chiral limit we determine $\kappa_c=0.1568(1)$ and $m_N a=0.531(13)$. Using the nucleon mass to set the scale to study nucleon properties [3,10,13], the lattice spacing $a^{-1}=1.76(4)$ GeV is determined. The four κ's then correspond to the tadpole improved lattice quark masses of about 376, 210, 124, and 80, MeV respectively [11,10]. Figure 2 shows the dipole fitting of $T_{CI}(q^2)$ at different q^2. Following the calculation for the point-split Wilson current [10], the tadpole improvement factor $1/8\kappa_c\langle\frac{1}{3}\mathrm{Tr}\,U_{plaq}\rangle^{1/4}$ ($\kappa_c=0.15684$) is included in the unrenormalized $J_{q,CI}$. The chiral limit for $J_{q,CI}$ is taken from a linear dependence on the quark mass $m_q a$ for these four κ values (see Fig. 3). To account for the correlations, both the dipole fitting and the chiral extrapolation are done with the covariance matrix and the final error at the chiral limit is obtained from the jackknife procedure. The dipole mass is found to be 0.88 ± 0.07 GeV. Finally, to obtain the result in the modified minimal subtraction scheme ($\overline{\mathrm{MS}}$) scheme at $1/a=1.76$ GeV (the scale is determined from the nucleon mass), we multiply the $J_{q,CI}$ by the tadpole improved renormalization constant for the operator T_{4j} which has been calculated [12] perturbatively to be $Z=1.045$ and obtain the CI part of the quark angular momentum $J_{q,CI}=0.44\pm0.07$. Being $\sim$90% of the nucleon spin, this almost saturates the spin

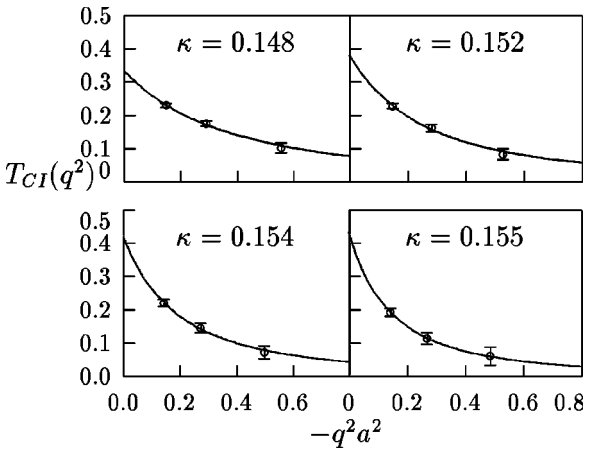

FIG. 2. Dipole fitting for $T_{CI}(q^2)$ at 4 different κ values.

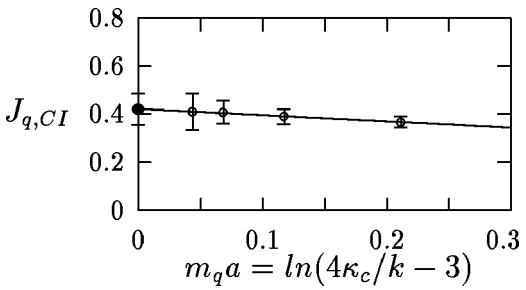

FIG. 3. Chiral extrapolation for $J_{q,CI}$ as a function of the quark mass. The value at the chiral limit is indicated by ●.

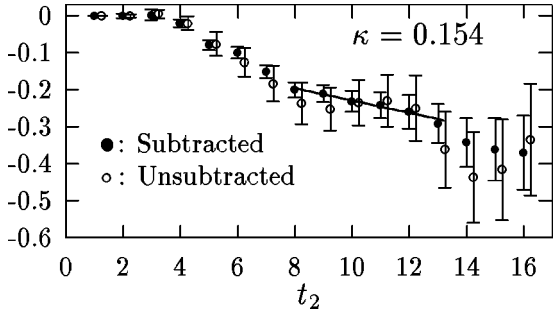

FIG. 4. The summed ratios of Eq. (5) for the DI are plotted for different time slice t_2 with and without unbiased subtraction. Ratios without subtraction are shifted slightly towards the right.

sum rule. We also performed monopole fitting for the $T_{CI}(q^2)$ and found an order of magnitude larger χ^2. The calculation is done on a quenched $16^3\times 24$ lattice at $\beta=6.0$ with Wilson fermions for 100 configurations.

For the DI contribution, we follow the calculations for the flavor-singlet axial coupling [3], the $\pi N\sigma$ term [13], and the strangeness magnetic moment [14] by summing the current insertion time t_1 from the nucleon source to its sink in the corresponding ratio in Eq. (5) for the DI [Fig. 1(b)] to gain statistics. In this case, the ratio leads to const $+1/2\epsilon_{jkm}q_k T_{DI}(q^2)\,t_2$. We take the average of the 3 polarization directions. The DI result is calculated from the slope of this summed ratio with respect to t_2. To evaluate the trace of the quark loop in Fig. 1(b), we adopt the same stochastic algorithm with the Z_2 noise estimator [15] as in other DI calculations [3,13,14]. In addition, we shall use two more techniques to reduce the errors from the stochastic algorithm. First one is to observe that from the charge conjugation and Euclidean Hermiticity (CH symmetry), the three-point function for the DI which is the product of the quark loop and the nucleon propagator is real. On the other hand, the Euclidean Hermiticy itself dictates that the loop should also be real. Therefore, we need only multiply the real part of the loop with the real part of the nucleon propagator and neglect the product of the imaginary parts of them which only introduces noise to the signal. Secondly, we employ an unbiased subtraction method which has been used in the calculation of the fermion determinant [16]. The trace of the inverse matrix A^{-1} can be estimated stochastically as follows:

$$\mathrm{Tr}(A^{-1})=E\left[\left\langle \eta^{\dagger}\left(A^{-1}-\sum_{i=1}^{P}\lambda_i O^{(i)}\right)\eta\right\rangle\right], \qquad (6)$$

where η's are Z_2 noise vectors, $O^{(i)}$'s are a set of P traceless matrices, and λ_i's are the variational parameters which are determined by reducing the variance of the three-point function over the gauge configurations. In practice, we found that a judicious choice of $O^{(i)}$ is a set of traceless matrices from the hopping expansion of the propagator. Since they match the off-diagonal behavior of the matrix A^{-1}, they can offset the off-diagonal contribution to the variance [16]. This method proves to be very efficient in reducing the error of the DI calculation with negligible overhead. After implementing the CH and H symmetries and the unbiased subtraction with traceless matrices obtained from just the first two terms of the hopping expansion, we obtain a reduction of error of 3–4 times.

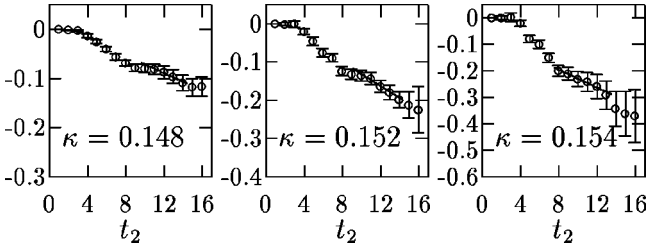

FIG. 5. The summed ratios of Eq. (5) for the DI are plotted for $|\vec{q}|=2\pi/La$.

Figure 4 shows a plot of the summed three-point to two-point function ratio [as in Eq. (5) for the DI] vs t_2 for $\kappa=0.154$ and $|\vec{q}|=2\pi/La$ with and without subtraction. One can see that the error bars before subtraction are much larger and only with the subtraction does one get a reasonably good slope as illustrated by the fitted straight line. With the help of this subtraction procedure we calculate slopes for other q^2 and for other κ's which are shown in Fig. 5. We use fixed source and vary the sink position t_2. From $t_2=8$ on, the nucleon becomes isolated from its excited states [10]. Hence, the slopes are fitted in the region $t_2\geqslant 8$ (Fig. 5) to avoid contamination from the excited states as was done previously [3,13,14]. Next, $T_{DI}(q^2)$ is fitted with a monopole form in q^2 as in the other DI calculations [13,14]. These are plotted in Fig. 6. Similar to the CI case, we also use covariant matrix fitting and the final error bars are obtained by the jackknife method. A finite mass correction factor from the triangle diagram [17] is introduced while extrapolating to the chiral limit with a linear $m_q a$ dependence. This is shown in Fig. 7(a). The strange quark contribution is obtained by fixing the disconnected sea quark mass at $\kappa_s=0.154$ and extrapolate the valence κ_v from 0.148,0.152,0.154 to κ_c. This is shown in Fig. 7(b). It is interesting to point out that the result is fairly independent of the sea quark mass in the fermion loop [Fig. 1(b)]. Comparing Fig. 7(a) where the valence and disconnected sea quarks are kept the same ($\kappa_v=\kappa_s$) and Fig. 7(b), we see that albeit the disconnected sea quark mass in Fig. 7(a) changes by a factor of 3, the result still coincides with those in Fig. 7(b) for each of the valence-quark cases. This shows that the DI depends on the valence-quark mass but is almost independent of the mass of the sea quarks in the fermion loop.

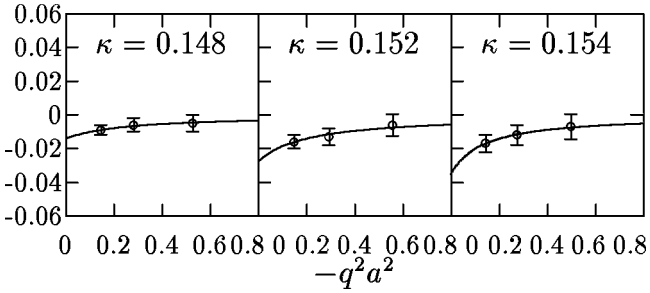

FIG. 6. Monopole fitting for $T_{DI}(q^2)$. $T_{DI}(0)$ values are obtained by extrapolating to $q^2\to 0$.

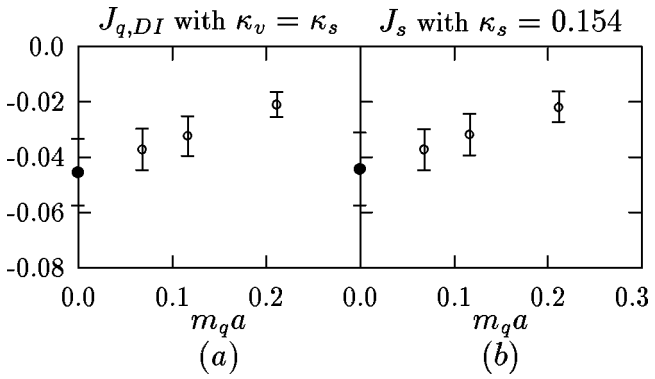

FIG. 7. (a) The lattice $J_{q,DI}$ as a function of the quark mass $m_q a$. The quark masses in the valence and the disconnected sea are kept the same. (b) J_s vs the valence quark mass with the disconnected sea quark mass fixed at $\kappa_s = 0.154$. The chiral limit value ($\kappa_v = \kappa_c$) is indicated by ●.

This is reminiscent of the disconnected sea-quark contribution in the flavor-singlet g_A^0 calculation [3] where the disconnected sea-flavor independence was first observed.

The breakdown of the quark angular momentum J_q into the quark spin $\frac{1}{2}\Sigma$ and the quark orbital angular momentum at the $\overline{\text{MS}}$ scale of 1.76 GeV is given in Table I. From the CI calculation we obtain the valence and connected sea quark contributions to the quark angular momentum $J_{q,CI} = 0.44 \pm 0.07$ which is $\sim 90\%$ of the total proton spin and it almost saturates the spin sum rule in Eq. (1) by itself. A previous calculation of the flavor-singlet axial current on the same set of lattices shows that $\frac{1}{2}\Sigma_{CI} = 0.31 \pm 0.04$ [3]. Since $J_{q,CI} = \frac{1}{2}\Sigma_{CI} + L_{q,CI}$, we obtain the CI part of the quark orbital angular momentum $L_{q,CI} = 0.13 \pm 0.07$. Thus, for valence and connected sea quarks in the CI [19], about 70% of $J_{q,CI}$ comes from the quark spin and the 30% is due to the orbital angular momentum. From the DI calculation, we find that the total quark angular momentum $J_{q,DI}$, like the quark spin $\frac{1}{2}\Sigma_{DI}$, is also flavor symmetric within errors. In fact, $J_{u,DI}$, $J_{d,DI}$, and J_s are all equal to -0.047 ± 0.012. Together, the total DI is $J_{q,DI} = -0.14 \pm 0.04$. Subtracting the DI of the quark spin $\frac{1}{2}\Sigma_{DI} = -0.18 \pm 0.03$ from $J_{q,DI}$, we obtain the orbital angular momentum contribution from the disconnected sea quarks to be $L_{q,DI} = 0.041 \pm 0.035$. It is interesting to note that it is consistent with zero with a central value which is a factor of 4.5 smaller than the spin content of the disconnected sea quarks. Adding CI and DI contributions together, we obtain $J_q = 0.30 \pm 0.07$ and, thus, we predict the gluon angular momentum $J_g = 0.5 - 0.30 \pm 0.07 = 0.20 \pm 0.07$ from the spin sum rule [Eq. (1)].

We should point out that the above results are obtained on lattice configurations with one coupling ($\beta = 6.0$) without extrapolation to the continuum. As such, it is expected to have $O(a)$ error in scaling violation in general for the Wilson fermions used in this work. However, a recent study of the iso-vector axial coupling constant, g_A^3 at three couplings [18] shows the dimensionless quantity g_A^3 has an $O(a^2)$ dependence on the lattice spacing a. As a result of this milder dependence on a, the g_A^3 when extrapolated to the continuum is only larger than the one at $\beta = 6.0$ by $\sim$ 6%. Since our results are obtained at $\beta = 6.0$ and, like g_A^3, the quark angular momentum J_q is dimensionless and contains the flavor-singlet g_A^0 as a part, we expect the error of the present results to be of the same order, i.e., 6% as far as the scaling violation is concerned.

TABLE I. The breakdown of quark angular momentum.

	J_q	$\frac{1}{2}\Sigma$	L_q
$u+d(CI)$	0.44(7)	0.31(4)	0.13(7)
$u/d(DI)$	−0.047(12)	−0.062(6)	0.015(12)
s	−0.047(12)	−0.058(6)	0.011(12)
$u+d+s(DI)$	−0.14(4)	−0.18(3)	0.041(36)
Total	0.30(7)	0.13(6)	0.17(6)

IV. CONCLUSIONS

To conclude, the total angular momentum of the quarks is calculated on the quenched $16^3 \times 24$ lattice at $\beta = 6.0$ to be $J_q = 0.30 \pm 0.07$ at the $\overline{\text{MS}}$ scale of 1.76 GeV, i.e., $\sim 60\%$ of the proton spin is attributable to the quarks. Since the quark spin content is calculated previously to be $\frac{1}{2}\Sigma = 0.13 \pm 0.06$ [3] on the same lattice configurations, we obtain the quark orbital angular momentum $L_q = 0.17 \pm 0.06$. Therefore, about 25% of the proton spin originates from the quark spin and about 35% comes from the quark orbital angular momentum. The gluon angular momentum contribution is predicted from the spin sum rule to be $J_g = 0.20 \pm 0.07$, i.e., $\sim$ 40% of the proton spin is due to the glue. Since the orbital angular momentum of the disconnected sea quarks turns out to be quite small, the flavor independence of $J_{q,DI}$ reconfirms the sea flavor independence of the quark spin in the DI, namely $\Delta u(DI) = \Delta d(DI) \simeq \Delta s$ observed in the previous lattice calculation [3].

In addition, the fact that $J_{q,CI}$ almost saturates the spin sum rule and the disconnected sea quark orbital angular momentum is small, the gluon angular momentum and the disconnected sea quark spin largely cancel each other. Both the flavor independence in the DI and the cancellation between the gluon angular momentum and the disconnected sea quark spin suggest that it is related to the anomaly and anomalous chiral Ward identity.

It is important for future experiments to measure the quark orbital angular momentum and the gluon angular momentum in order to conclude the study of the spin and content of the proton. The present work is based on the quenched approximation. It is also subjected to the large volume, finite lattice spacing, and chiral extrapolation corrections which can be as large as 20–30 % [3,13] and will be addressed in future studies with overlap fermions [20,21].

ACKNOWLEDGMENTS

This work is partially supported by DOE Grant No. DE-FGO5-84ER40154, DE-FG02-88ER40448, NSF Grant No. 9722073, and KBN Grant No. 2 P03B 011 19. We thank X. Ji for fruitful discussions.

[1] For recent reviews, see, for example, H. Y. Cheng, Int. J. Mod. Phys. A **11**, 5109 (1996); B. Lampe and E. Reya, Phys. Rep. **332**, 1 (2000).
[2] J. Ashman *et al.*, Phys. Lett. B **206**, 364 (1988); D. Adams *et al.*, Phys. Rev. D **56**, 5330 (1997); K. Abe *et al.*, *ibid.* **58**, 112003 (1998).
[3] S. J. Dong, J.-F. Lagaë, and K. F. Liu, Phys. Rev. Lett. **75**, 2096 (1995); M. Fukugita, Y. Kurumashi, M. Okawa, and A. Ukawa, *ibid.* **75**, 2092 (1995); SESAM Collaboration, S. Güsken *et al.*, Phys. Rev. D **59**, 114502 (1999).
[4] L. M. Sehgal, Phys. Rev. D **10**, 1663 (1974).
[5] P. G. Ratcliffe, Phys. Lett. B **192**, 180 (1987); X. Ji, J. Tang, and P. Hoodbhoy, Phys. Rev. Lett. **76**, 740 (1996).
[6] T. P. Cheng and L. F. Li, Phys. Rev. D **57**, 344 (1998); X. Song, hep-ph/9802206.
[7] J. Ellis and M. Karliner, Phys. Lett. B **213**, 73 (1988).
[8] X. Ji, Phys. Rev. Lett. **78**, 610 (1997); **79**, 1225 (1997).
[9] K. F. Liu *et al.*, Phys. Rev. D **59**, 112001 (1999).
[10] K. F. Liu, S. J. Dong, T. Drapper, J. M. Wu, and W. Wilcox, Phys. Rev. D **49**, 4755 (1994).
[11] G. P. Lepage and P. Mackenzie, Phys. Rev. D **48**, 2250 (1993).
[12] S. Capitani *et al.*, hep-lat/9711007.
[13] S. J. Dong, J.-F. Lagaë, and K. F. Liu, Phys. Rev. D **54**, 5496 (1996).
[14] S. J. Dong, K. F. Liu, and A. G. Williams, Phys. Rev. D **58**, 074504 (1998).
[15] S. J. Dong and K. F. Liu, Phys. Lett. B **328**, 130 (1994).
[16] C. Thron, S. J. Dong, K. F. Liu, and H. P. Ying, Phys. Rev. D **57**, 1642 (1998).
[17] J.-F. Lagaë and K. F. Liu, Phys. Rev. D **52**, 4042 (1995).
[18] S. Capitani *et al.*, Nucl. Phys. B (Proc. Suppl.) **79**, 548 (1999).
[19] K. F. Liu, Phys. Rev. D **62**, 074501 (2000).
[20] H. Neuberger, Phys. Lett. B **417**, 141 (1998); *ibid.* **427**, 353 (1998).
[21] K. F. Liu, S. J. Dong, F. Lee, and J. B. Zhang, Nucl. Phys. B (Proc. Suppl.) **83**, 636 (2000); hep-lat/0006004.